



Published in final edited form as:

Langmuir. 2010 June 1; 26(11): 8008–8014. doi:10.1021/la904903g.

Magnetic Barcoded Hydrogel Microparticles for Multiplexed Detection

Ki Wan Bong, Stephen C. Chapin, and Patrick S. Doyle*

Department of Chemical Engineering, Massachusetts Institute of Technology, 77 Massachusetts Avenue, Cambridge, MA 02139 (USA)

Abstract

Magnetic polymer particles have been used in a wide variety of applications ranging from targeting and separation to diagnostics and imaging. Current synthesis methods have limited these particles to spherical or deformations of spherical morphologies. In this paper, we report the use of stop flow lithography to produce magnetic hydrogel microparticles with a graphical code region, a probe region, and a magnetic tail region. These anisotropic multifunctional magnetic polymer particles are an enhanced version of previously synthesized “barcoded” particles [ref. 33] developed for the sensitive and rapid multiplexed sensing of nucleic acids. The newly added magnetic region has acquired dipole moments in the presence of weak homogeneous magnetic fields, allowing the particles to align along the applied field direction. The novel magnetic properties have led to practical applications in the efficient orientation and separation of the barcoded microparticles during biological assays without disrupting detection capabilities.

Introduction

Magnetic polymer particles consist of magnetically addressable components entrapped within or coated on a polymer matrix that can be precisely tuned to exhibit a range of desired physical and chemical properties. This powerful combination of functionality and customization has enabled the use of such particles in biomedical applications¹⁻⁴, microscale assembly⁵⁻⁸, structural color printing⁹, imaging¹⁰, and purification technology¹¹. In addition, the particles have been employed in microfluidic channels for bioassays¹²⁻¹⁵, mixing¹⁶⁻¹⁸, trapping¹⁹, transporting²⁰, and separation²¹⁻²⁵. Recently, biological entities including cells and aptamers were labeled with magnetic polymer particles and subsequently separated in a spatially-addressable sorting manner by generating magnetic field gradients in microfluidic channels^{26, 27}.

The enormous potential of magnetic polymer particles has fueled the development of several distinct synthesis methods. The conventional emulsification methods based on homogenization use shear forces to encase superparamagnetic nanoparticles of metal oxides within polymer droplets²⁸. Unfortunately, these approaches produce droplets with a wide size distribution and consume large amounts of energy²⁸. Membrane²⁹ and microchannel emulsifications³⁰⁻³² have been introduced as alternative methods that can provide higher degrees of monodispersity for a fraction of the energy cost. Microchannel emulsification in particular has produced anisotropic magnetic gel particles using channel geometries³⁰ or a double emulsion technique³¹. Janus superparamagnetic gel particles have also been generated with this approach³². However, the above methods have limited the particle morphologies to spheres or

*pdoyle@mit.edu

deformed spheres²⁸⁻³². A more flexible synthesis system would expand the possible geometries and thereby augment the applicability of the magnetic polymer particles produced.

Encoded microparticles have been suggested as diagnostic tools for the rapid, multiplexed screening of biomolecules due to their advantages in detection and quantification³³⁻³⁵. Compared to traditional planar arrays, particle-based arrays offer easier probe-set modification, more efficient mixing steps, and higher degrees of reproducibility. While polymer microspheres doped with fluorescent dyes have been used most extensively³⁶, there are numerous systems under development that employ chemical, graphical, electronic, or physical encoding schemes for use in multiplexed detection³⁴. Microcarriers fabricated from a variety of advanced materials such as inverse-opaline photonic beads³⁷ have the potential to transform the biodiagnostic field by enabling the analysis of complex sample media (such as serum), eliminating the need for costly and time-consuming labeling steps, and lowering limits of detection.

Barcoded hydrogels are an emerging subclass of encoded particles that exhibit higher sensitivities and more favorable hybridization kinetics than common metallic and polystyrene microparticles that immobilize probe species on solid surfaces³⁸. To capture target molecules and report interaction information in multiplexed analysis, each anisotropic particle bears a probe region and a corresponding graphical code region that identifies the probe species. Production of these particles requires a novel synthesis method called stop flow lithography (SFL)³⁹, which affords precise control over morphology and functionality through the semi-continuous photopolymerization across coflowing laminar streams of various chemical compositions in microfluidic channels. While the resulting gel-based particles have proven to be effective tools in past multiplexed sensing of DNA and RNA, their use in suspension assays and other screening processes would be greatly simplified with the introduction of an appropriate means for addressing and aligning the particles during rinsing, mixing, and analysis procedures.

Magnetic barcoded particles are now introduced as an enhanced version of hydrogel microparticles for suspension assays that can be manipulated using magnetic fields. Through a slight modification of the SFL technique³⁹, it is now possible to incorporate magnetically addressable entities within a specific region of the microparticles. Particles synthesized with a magnetic tail region respond to weak magnetic fields, while still maintaining the ability to sensitivity and specifically detect oligonucleotide targets in solution. The advantages of the magnetic tail are demonstrated through directed orientation as well as bulk separation using a magnet.

Experimental

Materials

All particles shown in this work were made from poly(ethylene glycol) (700) diacrylate (PEG-DA 700, Sigma Aldrich). The code regions were synthesized using prepolymer solutions of 35% (v/v) PEG-DA 700, 20% poly(ethylene glycol) (200) (PEG 200, Sigma Aldrich), 5% Darocur 1173 (Sigma Aldrich) initiator, and 40% 3× Tris-EDTA (pH =8.0, EMD) buffer. Rhodamine acrylate (Sigma Aldrich) and food coloring (Tone Brothers Inc.) were mixed into the prepolymer solutions for the code to give final concentrations of 0.4% and 2%, respectively. The composition of prepolymer for the probe regions was 20% PEG-DA 700, 40% PEG 200, 5% Darocur 1173, and 35 % 3× Tris-EDTA buffer. Oligonucleotide probes, #1 (5'-ATA GCA GAT CAG CAG CCA GA-3') and #2 (5'-CAC TAT GCG CAG GTT CTC AT-3'), were purchased from IDT with acrydite modifications on the 5' end and mixed into the probe prepolymer to give a final concentration of 50 μM. Lastly, the magnetic region was prepared using solutions of 35% PEG-DA 700, 5% Darocur 1173, and 60 % magnetic bead solutions

(Seradyn Inc., carboxylate-modified, 5% solids). Prior to being incorporated into the particles, the commercial superparamagnetic beads exhibited a short response time upon the introduction of a magnetic field and had uniform size ($779 \text{ nm} \pm 10\%$, diameter)⁴⁰. Using alternating gradient magnetometry (AGM, MicroMag™ 2900), the measured saturation magnetization values for the beads (dried) and the magnetic regions (dried) of barcoded particles were found to be 28 emu/g and 3 emu/g, respectively (Supporting Information). As the mass of each barcoded microparticle varied depending on the code design, we polymerized particles consisting of only a magnetic region and measured the magnetization value for these simple hydrogels. A perfusion solution consisting of PEG-DA 700 was also used to move unincorporated magnetic beads into a waste reservoir to prevent the excess beads from sticking to the probe and code regions of the synthesized particles.

Microfluidic Devices

Microfluidic devices were generated by pouring PDMS (mixed at a base-to-curing agent ratio of 10:1) over an SU-8 master and then curing 2 hr at 60 °C in an oven. In each device, the particle synthesis chamber was 300 μm in width and 20 μm in height, while the perfusion channel was 70 μm in width and 110 μm in height. Each device was placed on a PDMS-coated glass slide and then sealed by curing overnight at 60 °C in an oven. For synthesis, devices were mounted on an inverted microscope (Axiovert 200, Zeiss) equipped with a VS25 shutter system (UniBlitz) to precisely control the UV exposure dose³⁹. A reservoir was cut into the PDMS to collect the particles.

Stop Flow Lithography Setup

We generated controlled pressures in the range of 0–15 psia from house air using a Type 100 LR manual pressure regulator (Controlair Inc.). Downstream of the regulator, a 3-way solenoid valve (Burkert) was used to switch rapidly between atmospheric pressure (stop) and the input pressure (flow). The output from the 3-way valve was connected to 200 μl pipette tips (Molecular BioProducts) using rubber tubing (Tygon). The pipette tips were filled with $\sim 100 \mu\text{l}$ of the desired prepolymer solution and inserted into the channel inlet ports. The 3-way valve and above shutter were controlled using a custom written script in Labview 8.1 (National Instruments).

Photopolymerization Setup

Photomasks were designed in AUTOCAD 2005 and printed using a high-resolution printer at CAD Art Services (Bandon, OR). The mask was then inserted into the field-stop of the microscope. A Lumen 200 (Prior) served as the source of UV light, and a filter set that allowed wide UV excitation (11000v2: UV, Chroma) was employed to provide light of the desired wavelength for synthesis. The UV exposure time was limited to 75 ms using the automated shutter system.

Magnetic Responsiveness

To investigate the response of the magnetic barcoded particles in the presence of an external magnetic field, we fabricated analysis reservoirs by sealing a PDMS rectangular frame ($5 \times 5 \times 5 \text{ mm}$) onto a PDMS-coated glass slide. Each reservoir was filled with the magnetic barcoded particles suspended in deionized water with 0.005% (v/v) Tergitol NP-10 (Sigma Aldrich, St. Louis, MO) (to ensure there is no microparticle aggregation) and then placed in a uniform magnetic field (planar or normal) induced by an electromagnetic coil connected to a DC power supply (GPS-2303, GWInsteck). The magnetic fields were calibrated using a Gauss meter (SYPRIS) with an axial probe (for the normal induced magnetic field) or a transverse probe (for the planar induced field).

Hybridization and Labeling

Incubation mixtures were prepared by adding ~ 50 particles of each desired type to a 0.65 mL Eppendorf tube containing a hybridization buffer of 0.5 M NaCl in TET (1× Tris-EDTA with 0.05% Tween-20 (Sigma Aldrich)). Particles were incubated with either 0 or 200 amol of two different biotinylated target oligonucleotides at 50 °C for 90 min using a thermomixer (Quantifoil Rio) with a mixing speed of 1800 rpm. Following hybridization, the samples were rinsed twice with 450 µl TET and then twice with 450 µl PBST (1× PBS (Cellgro) with 0.05% Tween-20). Then, the probe-target complexes were labeled by adding streptavidin-phycoerythrin (SAPE) diluted 1:500 in TET to the Eppendorf tube. The labeling process was carried out at 21.5 °C for 45 min with mixing at 1500 rpm in a Multi-Therm shaker (Biomega). Before imaging, the particles were rinsed three times with 450 µl TET and then twice with 450 µl PTET (5× Tris-EDTA buffer with 25% PEG 200 and 0.05% Tween-20).

Imaging for Quantitative Analysis

A 15-µl droplet containing ~ 20 particles was pipetted onto a glass slide and sandwiched for analysis using an 18 × 18 mm coverslip. The sample was mounted on a Zeiss Axiovert 200 microscope equipped with a UV Illumination source (X-Cite series 120, Exfo), and a custom macro in NIH Image was used to capture ten sequential frames from an EB-CCD camera (C7190-20, Hamamatsu) mounted to the side port of the microscope. Each frame had an exposure time of 1/33 sec, and the macro produced a final output image for analysis by averaging over the ten frames. Camera settings of 10, 1.6, and 9.9 for gain, offset, and sensitivity, respectively, were used. Images were analyzed using Image J.

Results and Discussion

Figure 1A shows a schematic depicting the synthesis of magnetic barcoded particles. Different prepolymer mixtures are infused into the three inlets, thereby generating stable three-phase laminar flows. The middle stream is composed of polyethylene glycol diacrylate (PEG-DA) with an acrylate modified DNA probe, while the top and bottom streams consist of PEG-DA with a fluorescent dye, rhodamine acrylate (rhodamine A), and with magnetic beads, respectively. The flows can be stopped via pressure release, during which an array of magnetic barcoded particles are formed by a 75 ms UV exposure through a transparency mask using a standard fluorescence microscope. A pressure pulse is then used to advect the polymerized particles into a collection reservoir. This process is repeated using an automated setup, allowing for the high-throughput synthesis of particles (18,000 per hour) in a semi-continuous manner. Prior to collection in the reservoir, a perfusion stream with flow perpendicular to that in the synthesis chamber was used to move un-incorporated magnetic beads into a waste outlet. This technique was introduced to simplify the rinsing procedures. While the excess beads flowed into the perfusion line, the much larger encoded particles were only collected in the reservoir of the synthesis chamber. The commercially available superparamagnetic beads were well-mixed with PEG monomer solutions and well-dispersed in microfluidic channels (Fig. 1B). Aside from the addition of the simple perfusion stream, no special processing steps or chemical treatments were required to integrate the magnetic streams into the SFL process.

The magnetic barcoded particles were comprised of three distinct regions: (1) code region for identifying particle and probe embedded within, (2) probe region for detecting target, and (3) magnetic region for providing magnetic addressability. The dimensions of each region were 105 × 70 µm, 55 × 70 µm, and 90 × 70 µm, successively (Fig. 1C). The size (0, 1, 2, and 3) and order of unpolymerized holes in the wafer structure were used to construct a graphical code to distinguish particle types. The number “0” was designed as a non-punched area, while the punched dimensions of numbers “1”, “2”, and “3” were 12 × 15 µm, 12 × 27.5 µm, and 12 × 40 µm, respectively. Careful focusing and inlet pressure control during the

photopolymerization process ensured a high degree of reproducibility in the creation of the coding holes and the different chemical regions on each microparticle.

Figure 2 contains images of the synthesized magnetic barcoded particles. As seen in brightfield images (Fig. 2A, C and E), the brown magnetic regions are clearly separated from the neighboring probe regions. Well-developed code regions are shown in fluorescent images (Fig. 2B and D), with sharp interfaces and feature resolution provided by the SFL process. We prepared magnetic barcoded particles $\sim 16 \mu\text{m}$ in height by using $20 \mu\text{m}$ -high channels (Fig. 2C). The difference between particle and channel heights can be attributed to the $\sim 2 \mu\text{m}$ -thick oxygen inhibition layer on both the top and bottom channel surfaces⁴¹. Compared to code and probe regions, it was observed that the magnetic region was slightly thinner due to UV absorption by the iron oxide cores of the magnetic beads.

To investigate magnetic response, we exposed the magnetic barcoded particles dispersed in a 0.005% (v/v) aqueous Tergitol NP-10 solution in a PDMS reservoir to a weak homogeneous field ($21.1 \pm 0.1 \text{ mT}$) perpendicular to the reservoir substrate. Suspended in a non-magnetic medium, the particles acquired dipole moments and flipped up perpendicular to the plane, forming columnar structures along the applied field direction (Fig. 3A and Supporting Information). In the presence of a weak homogeneous field ($14.7 \pm 0.1 \text{ mT}$) parallel to the substrate plane, attractive induced dipolar interactions lead to tail-to-tail self assembly of the particles (Fig. 3B).

The magnetic functionality can be used to orient and transport the barcoded particles as shown in Figure 3C-E. Using a hand magnet, it was possible to remotely and precisely manipulate the orientation of magnetic barcoded particles at the inlet of a microfluidic channel to aspirate all particles such that they proceeded down the analysis chamber in a “probe first” (versus “code first”) orientation. Figure 3C shows the reorientation process of a barcoded particle from “code first” to “probe first” within a microfluidic channel. By moving a more powerful magnet even closer to the channel, it was possible to then transport this reoriented particle from the inlet to a more narrow zone used for single-particle analysis (Fig. 3D). Although the transportation velocity was only $10 \mu\text{m/s}$ in this experiment, the process was performed in a simple manner using a common magnet. This pumpless method for orientation and movement does not require the complex setup used in pressure-driven alignment processes and does not subject the soft hydrogel particles to the significant hydrodynamic forces that pressure-driven processes can introduce in microchannels⁴².

This capacity to address the position and orientation of individual particles provides a means for improving upon recently developed particle analysis methods. In particular, the fabrication of a magnetic aspiration column could be used to deliver all particles to a flow-through scanning chamber⁴² with the same probe-first orientation. As existing high-throughput flow alignment methods cannot control which end of the particle leads in the flow, decoding algorithms that determine probe identity and amount of bound target must additionally ascertain the orientation of the particle for accurate analysis. This requires using one of the coding elements as an orientation marker. If all particles could be magnetically addressed to give the same orientation prior to entrance into the flow chamber, this would no longer be necessary and the coding capacity of these microparticles could be expanded by a factor of four. It should also be noted that the simultaneous reorientation and transportation of multiple barcoded particles was achieved in a large reservoir using a hand magnet (Fig. 3E). This capability could potentially be exploited for the ordered presentation of post-hybridization particles in a plate-based stationary scan.

The magnetic functionality also introduces a new means by which the barcoded particles can be concentrated and subsequently separated from a carrier solution. In previous

implementations of barcoded hydrogel particles for biomolecule detection, ten centrifugal separations were required for the rinsing steps in a typical assay. This density-based separation strategy tends to concentrate fibers and other particulate matter along with the encoded microparticles at the bottom of the sample tube. If these contaminants then stick to the particles, they can interfere with the analysis of the fluorescence emitted by the code and probe regions. Magnetic force separation provides an alternative approach to segregating the barcoded particles for rinsing procedures. Using a permanent magnet, we successfully separated the particles on the side of a collection tube in 2 minutes (Fig. 3F). In further experiments, the ten rinsing steps of a DNA hybridization assay were carried out using magnetic barcoded hydrogel microparticles and only magnetic separation steps. Upon analysis of the particles, it was determined that the vast majority of particles had been retained and, furthermore, a considerably smaller amount of particulate matter was seen in the carrier solution.

A wide variety of geometrically and chemically complex magnetic barcoded particles can be prepared by SFL using simple mask replacements and inlet fluid exchanges. Table 1 summarizes the four particle types used in a multiplexed DNA sensing study, illustrating the code, the identity of incorporated probe, and the presence or absence of magnetic beads in the tail region. Types 1, 2, and 3 featured a magnetic tail and were incorporated with no probe (type 1), probe #1 (type 2), or probe #2 (type 3) in the central region. Type 4 featured a non-magnetic tail, bore probe #1, and was used to investigate the effect of the added magnetic material on target detection. If the magnetic region is indeed inert with respect to target capture, the mean signals from the target panels on types 2 and 4 should be the same when incubated with target corresponding to probe #1.

The four particle types were hybridized with either 0 or 200 amol of two different biotinylated target oligonucleotides. Following hybridization and labeling with SAPE, the fluorescent images of five particles of each type for each incubation condition were analyzed. An incubation matrix was prepared to compare the performance of the various particles (Fig. 4). Each plot in the matrix represents the average signal of 5 scans of each particle type at the specified incubation condition. The mean fluorescent intensity across the width of the particle (vertical axis, A.U.) was calculated and then plotted at each lengthwise position (horizontal axis, pixels) along the particle. The fluorescent intensities in the probe and tail regions were crucial to evaluating the success of the detection and examining the effect of the magnetic regions. As illustrated by a comparison of the results from types 2 and 4 in Figure 4, the mean signals in these regions are similar whether the tail region is magnetic or non-magnetic, indicating that the magnetic material does not interfere with the sensitive and specific detection of the oligonucleotides.

It should be noted that target 1 generated a lower signal than target 2 when incubations were performed with all four types simultaneously in a single Eppendorf tube. The lower signal for target 1 can be attributed to the presence of two particle types (2 and 4) bearing probe 1 in the incubation mixture. Because of this redundancy, target 1 was spread over ~100 total particles per incubation, whereas target 2 was spread over only ~50 total particles per incubation. When the same amount of target 1 (200 amol) was incubated with ~50 particles of type 4 (probe 1, non-magnetic) *alone*, a signal (~63.2 AU) as high as that seen with the particles bearing probe 2 in the earlier assays was observed, thus confirming that the particle density led to the disparity in the original target levels (Supporting Information).

Conclusions

We have demonstrated that a modified form of SFL can be used to generate magnetic barcoded particles through the addition of a monomer stream containing superparamagnetic beads, as well as a perfusion rinse stream. The added magnetic region can acquire dipole moments in

the presence of low-strength homogeneous magnetic fields, allowing the particles to align along the applied field direction. The magnetic barcoded particles have exhibited an enhanced range of functionality, providing novel means for orientation and separation during biological assays. The magnetic region has no apparent negative effects on the sensitive and specific multiplexed sensing of oligonucleotide targets. Although we have demonstrated the creation and use of relatively simple magnetic barcoded particles, the flow lithographic process for loading magnetic materials described here can perhaps be combined with more complex, multidimensional synthesis strategies such as lock release lithography (LRL)⁴³ and hydrodynamic focusing lithography (HFL)⁴⁴ to produce microparticles with additional novel properties advantageous for self-assembly and biomolecule detection studies.

Supplementary Material

Refer to Web version on PubMed Central for supplementary material.

Acknowledgments

We gratefully acknowledge the support of grant R21EB008814 from the National Institute of Biomedical Imaging and Bioengineering, National Institutes of Health, Kwanjeong Educational Foundation, the MIT Deshpande Center, and the Singapore-MIT Alliance. We also thank Dr Ramin Haghgooe for kindly providing a SU-8 master, and Dr Chunghee Nam and Dr Youngman Jang for their assistances with alternating gradient magnetometry.

References

- [1]. Millman JR, Bhatt KH, Prevo BG, Velev OD. *Nat. Mater* 2005;4:98–102. [PubMed: 15608646]
- [2]. Lee D, Cohen RE, Rubner MF. *Langmuir* 2005;21:9651–9659. [PubMed: 16207049]
- [3]. Lee D, Cohen RE, Rubner MF. *Langmuir* 2007;23:123–129. [PubMed: 17190494]
- [4]. Voltairas PA, Fotiadis DI, Michalis LK. *J. Biomech* 2002;35:813–821. [PubMed: 12021001]
- [5]. Doyle PS, Bibette J, Bancaud A, Viovy JL. *Science* 2002;295:2237–2237. [PubMed: 11910102]
- [6]. Smoukov SK, Gangwal S, Marquez M, Velev OD. *Soft Matter* 2009;5:1285–1292.
- [7]. Helseth LE. *Langmuir* 2005;21:7276–7279. [PubMed: 16042453]
- [8]. Helseth LE, Muruganathan RM, Zhang Y, Fischer TM. *Langmuir* 2005;21:7271–7275. [PubMed: 16042452]
- [9]. Kim H, Ge J, Kim J, Choi S, Lee H, Lee H, Park W, Yin Y, Kwon S. *Nat. Photonics* 2009;3:534–540.
- [10]. Hoehn M, Kustermann E, Blunk J, Wiedermann D, Trapp T, Wecker S, Focking M, Arnold H, Hescheler J, Fleischmann BK, Schwindt W, Buhrlé C. *Proc. Natl. Acad. Sci. USA* 2002;99:16267–16272. [PubMed: 12444255]
- [11]. Berensmeier S. *Appl. Microbiol. Biotechnol* 2006;73:495–504. [PubMed: 17063328]
- [12]. Peyman SA, Iles A, Pamme N. *Lab Chip* 2009;9:3110–3117. [PubMed: 19823727]
- [13]. Hayes MA, Polson NA, Phayre AN, Garcia AA. *Anal. Chem* 2001;73:5896–5902. [PubMed: 11791558]
- [14]. Choi JW, Oh KW, Thomas JH, Heineman WR, Halsall HB, Nevin JH, Helmicki AJ, Henderson HT, Ahn CH. *Lab Chip* 2002;2:27–30. [PubMed: 15100857]
- [15]. Gijs MAM, Lacharme F, Lehmann U. *Chem. Rev.* 2009 10.1021/cr9001929.
- [16]. Rida A, Gijs MAM. *Appl. Phys. Lett* 2004;85:4986–4988.
- [17]. Biswal SL, Gast AP. *Anal. Chem* 2004;76:6448–6455. [PubMed: 15516140]
- [18]. Rida A, Gijs MAM. *Anal. Chem* 2004;76:6239–6246. [PubMed: 15516114]
- [19]. Lee CS, Lee H, Westervelt RM. *Appl. Phys. Lett* 2001;79:3308–3310.
- [20]. Deng T, Whitesides GM, Radhakrishnan M, Zabow G, Prentiss M. *Appl. Phys. Lett* 2001;78:1775–1777.
- [21]. Ostergaard S, Blankenstein G, Dirac H, Leistiko O. *J. Magn. Magn. Mater* 1999;194:156–162.
- [22]. Pamme N, Manz A. *Anal. Chem* 2004;76:7250–7256. [PubMed: 15595866]

- [23]. Pamme N. *Lab Chip* 2006;6:24–38. [PubMed: 16372066]
- [24]. Pamme N. *Lab Chip* 2007;7:1644–1659. [PubMed: 18030382]
- [25]. Zhang K, Liang QL, Ma S, Mu XA, Hu P, Wang YM, Luo GA. *Lab Chip* 2009;9:2992–2999. [PubMed: 19789755]
- [26]. Lou XH, Qian JR, Xiao Y, Viel L, Gerdon AE, Lagally ET, Atzberger P, Tarasow TM, Heeger AJ, Soh HT. *Proc. Natl. Acad. Sci. USA* 2009;106:2989–2994. [PubMed: 19202068]
- [27]. Adams JD, Kim U, Soh HT. *Proc. Natl. Acad. Sci. USA* 2008;105:18165–18170. [PubMed: 19015523]
- [28]. Yuan QC, Williams RA. *China Particuology* 2007;5:26–42.
- [29]. Vladislavjevic GT, Williams RA. *Adv. Colloid Interfac* 2005;113:1–20.
- [30]. Hwang DK, Dendukuri D, Doyle PS. *Lab Chip* 2008;8:1640–1647. [PubMed: 18813385]
- [31]. Chen CH, Abate AR, Lee DY, Terentjev EM, Weitz DA. *Adv. Mater* 2009;21:3201–3204.
- [32]. Yuet KP, Hwang DK, Haghgooie R, Doyle PS. *Langmuir*. 2009 DOI: 10.1021/la903348s.
- [33]. Pregibon DC, Toner M, Doyle PS. *Science* 2007;315:1393–1396. [PubMed: 17347435]
- [34]. Wilson R, Cossins AR, Spiller DG. *Angew. Chem. Int. Ed* 2006;45:6104–6117.
- [35]. Birtwell S, Morgan H. *Integr. Biol* 2009;1:345–362.
- [36]. Kellar KL, Douglass JP. *J. Immunol. Methods* 2003;279:277–285. [PubMed: 12969567]
- [37]. Zhao YJ, Zhao XW, Hu J, Xu M, Zhao WJ, Sun LG, Zhu C, Xu H, Gu ZZ. *Adv. Mater* 2009;21:569–572.
- [38]. Pregibon DC, Doyle PS. *Anal. Chem* 2009;81:4873–4881. [PubMed: 19435332]
- [39]. Dendukuri D, Pregibon DC, Collins J, Hatton TA, Doyle PS. *Nat. Mater* 2006;5:365–369. [PubMed: 16604080]
- [40]. <http://www.seradyn.com/technical/pdf/SpeedBeadsTN.pdf>
- [41]. Dendukuri D, Gu SS, Pregibon DC, Hatton TA, Doyle PS. *Lab Chip* 2007;7:818–828. [PubMed: 17593999]
- [42]. Chapin SC, Pregibon DC, Doyle PS. *Lab Chip* 2009;9:3100–3109. [PubMed: 19823726]
- [43]. Bong KW, Pregibon DC, Doyle PS. *Lab Chip* 2009;9:863–866. [PubMed: 19294294]
- [44]. Bong KW, Bong KT, Pregibon DC, Doyle PS. *Angew. Chem. Int. Ed* 2010;49:87–90.

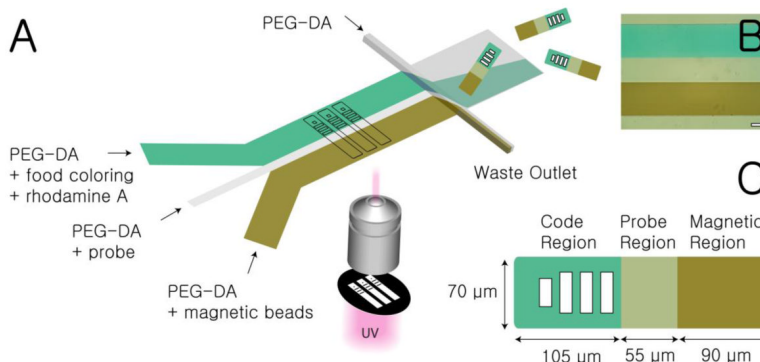


Figure 1. Production of magnetic barcoded particles. (A) Synthesis process of magnetic barcoded particles. Stop flow lithography (SFL) is used to generate particles with three distinct chemical regions. The top stream is comprised of PEG-DA with food coloring and rhodamine A, while the other streams consist of PEG-DA with probe oligonucleotide and magnetic beads, respectively. Downstream of the synthesis site, a PEG-DA perfusion stream is used to move un-incorporated magnetic beads into a waste outlet. (B) An experimental bright field image of the three phases flowing in the channel. The magnetic beads in the bottom flow are seen to be well-dispersed. The scale bar is $50\ \mu\text{m}$. (C) Dimensions of a magnetic barcoded particle. Coding holes are designed with the following dimensions: '1' ($12 \times 15\ \mu\text{m}$), '2' ($12 \times 27.5\ \mu\text{m}$), and '3' ($12 \times 40\ \mu\text{m}$). The code in this illustration is '2333'.

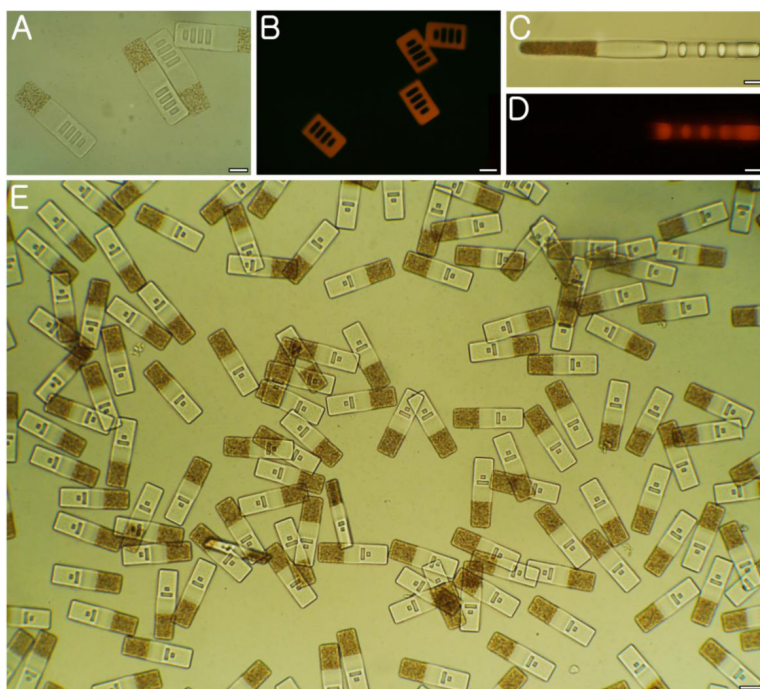


Figure 2. Magnetic barcoded particles. (A) A bright field image (20× objective) of magnetic barcoded particles with code '2333'. (B) A fluorescent image of (A). (C) The side view of a magnetic barcoded particle in a bright field image (20× objective). (D) A fluorescent image of (C). (E) A bright field image (5× objective) of magnetic barcoded particles with code '0013'. Scale bars are 50 μm (A and B), 25 μm (C and D) and 100 μm (E).

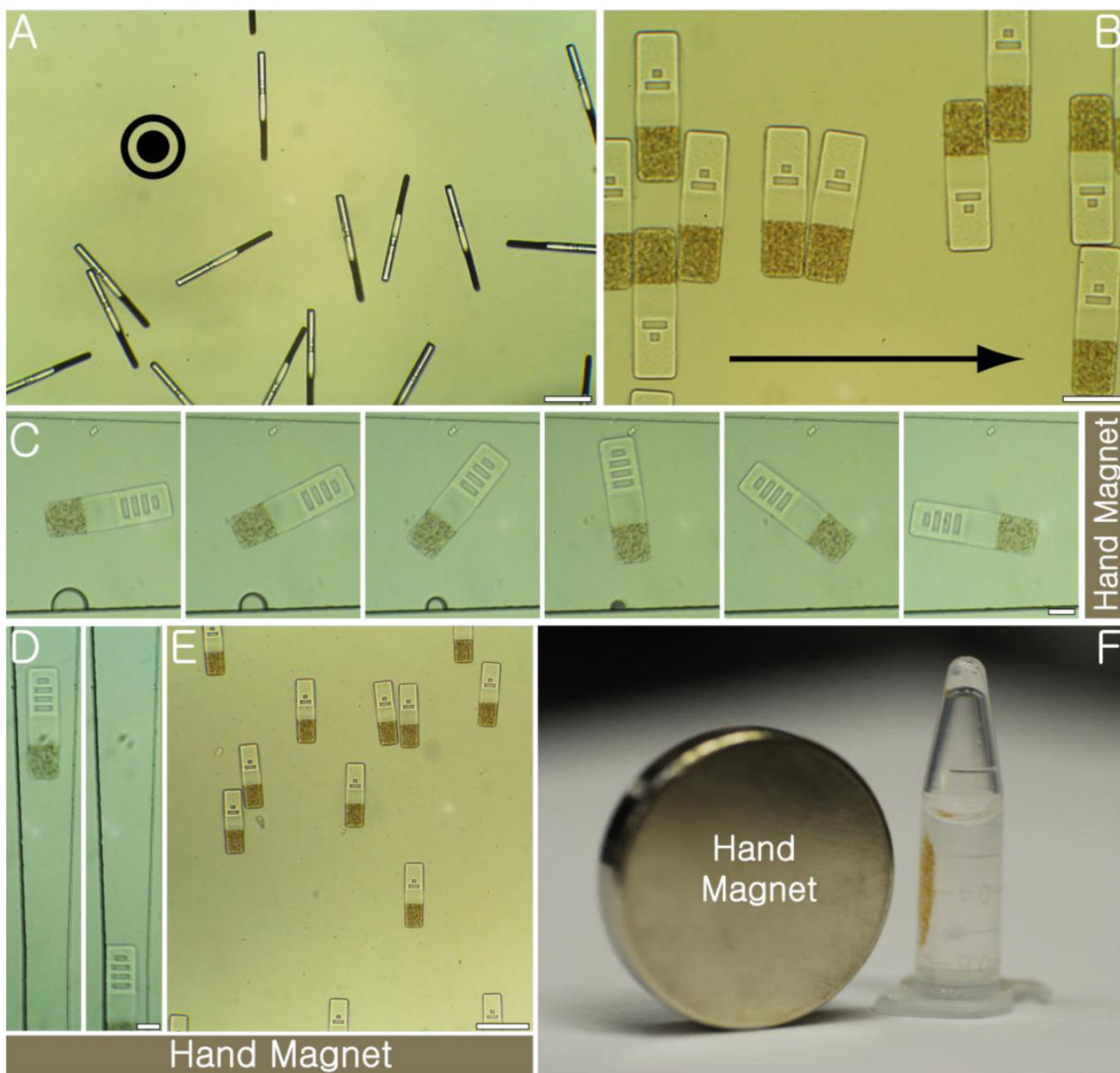


Figure 3.

Response of magnetic barcoded particles. (A) Response of magnetic barcoded particles to out-of-plane (21.1 ± 0.1 mT) magnetic field. (B) Response of magnetic barcoded particles to in-plane (14.7 ± 0.1 mT) magnetic field. (C) Reorientation of a magnetic barcoded particle in a microfluidic channel using a hand magnet. (D) Snapshots of magnetic transportation of a magnetic barcoded particle using a hand magnet. The particle was transported towards a narrow region in the microfluidic channel used for single-particle scanning analysis. (E) Image of reoriented magnetic barcoded particles moving towards a hand magnet. (F) Bulk separation of magnetic barcoded particles using a hand magnet. Scale bars are $50 \mu\text{m}$ (C and D), $100 \mu\text{m}$ (A and B), and $200 \mu\text{m}$ (E).

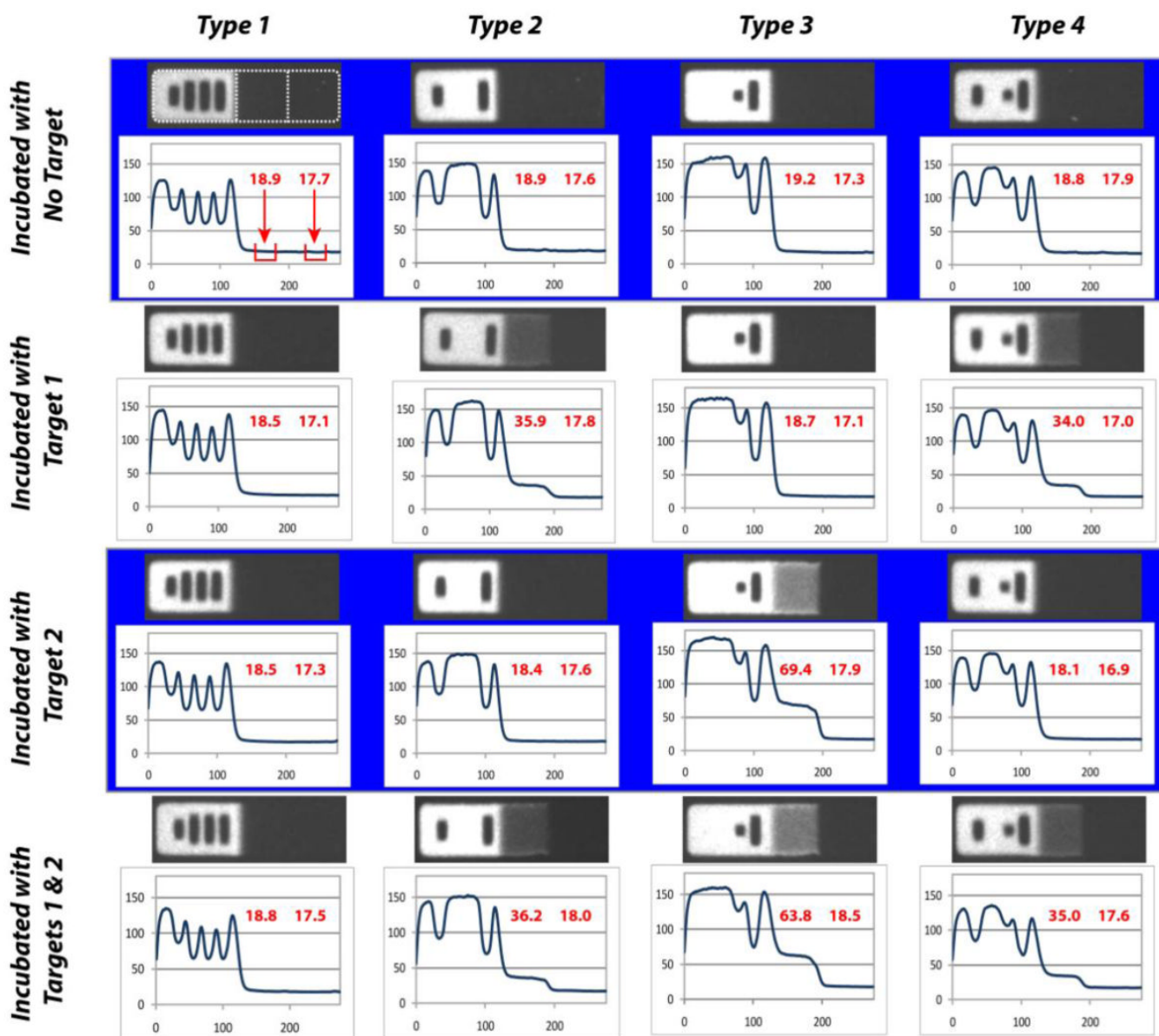
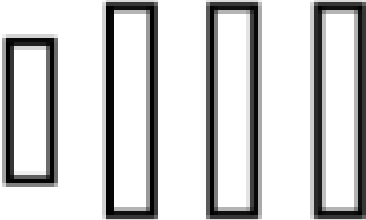


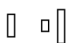


Figure 4. Incubation matrix. Particles with a fluorescent code region, an internal probe region, and a tail region were synthesized and incubated with either 0 or 200 amol of two different biotinylated target oligonucleotides at 50 °C for 90 min. Following incubation, probe-target complexes were labeled with streptavidin-phycoerythrin (SAPE) at 21.5 °C for 45 min. Particle type 1 featured no probe, a magnetic tail, and code '2333'; type 2 featured probe 1, a magnetic tail, and code '2003'; type 3 featured probe 2, a magnetic tail, and code '0013'; type 4 featured probe 1, a non-magnetic tail, and code '2013.' Each plot shows the average of 5 scans of each particle type under the specified incubation condition. Horizontal axis is axial (lengthwise) position in pixels, and vertical axis is mean fluorescent intensity in arbitrary units. The mean signal across the width of the particle has been computed and plotted at each axial position. The red numbers above each scan indicate the mean fluorescent intensity measured in the probe region and in the tail region. The red bars in the first plot indicate the windows over which the averages were taken. Quoted numbers represent the mean of five separate scans.

Table 1

Design of the four different magnetic barcoded particle types

Particle Type	Code		Pro
1	2333		No
2	2003		Prob
3	0013		Prob
4	2013		Prob